

Stoichiometrically graded SiNx for improved surface passivation in high performance solar cells

Keith T. Butler, John H. Harding, Machteld P. W. E. Lamers, and Arthur W. Weeber

Citation: J. Appl. Phys. 112, 094303 (2012); doi: 10.1063/1.4764012

View online: http://dx.doi.org/10.1063/1.4764012

View Table of Contents: http://jap.aip.org/resource/1/JAPIAU/v112/i9

Published by the American Institute of Physics.

Related Articles

Carrier escape mechanism dependence on barrier thickness and temperature in InGaN quantum well solar cells Appl. Phys. Lett. 101, 181105 (2012)

High performance radial p-n junction solar cell based on silicon nanopillar array with enhanced decoupling mechanism

Appl. Phys. Lett. 101, 183901 (2012)

First-principles study of point defects in solar cell semiconductor CuInS2 J. Appl. Phys. 112, 084513 (2012)

Addition of regiorandom poly(3-hexylthiophene) to solution processed poly(3-hexylthiophene):[6,6]-phenyl-C61-butyric acid methyl ester graded bilayers to tune the vertical concentration gradient APL: Org. Electron. Photonics 5, 235 (2012)

Addition of regiorandom poly(3-hexylthiophene) to solution processed poly(3-hexylthiophene):[6,6]-phenyl-C61-butyric acid methyl ester graded bilayers to tune the vertical concentration gradient Appl. Phys. Lett. 101, 173301 (2012)

Additional information on J. Appl. Phys.

Journal Homepage: http://jap.aip.org/

Journal Information: http://jap.aip.org/about/about_the_journal Top downloads: http://jap.aip.org/features/most_downloaded

Information for Authors: http://jap.aip.org/authors

ADVERTISEMENT



Stoichiometrically graded SiN_x for improved surface passivation in high performance solar cells

Keith T. Butler, ¹ John H. Harding, ¹ Machteld P. W. E. Lamers, ² and Arthur W. Weeber ² Department of Materials Science and Engineering, University of Sheffield, Mappin Street, Sheffield S1 3JD, United Kingdom

²ECN Solar Energy, NL-1755 ZG, Petten, The Netherlands

(Received 10 September 2012; accepted 3 October 2012; published online 1 November 2012)

The effects of an interface gradient in nitrogen concentration on a number of important properties of amorphous hydrogenated silicon nitride/crystalline silicon (a-SiN_x: H/c-Si) interfaces in the context of solar cell devices are investigated using molecular dynamics simulations. We simulate interfaces with a gradient of nitrogen which goes from SiN_{1,2} to Si over widths from 2 to 9 nm, in the presence of 10 at. % hydrogen, to recreate the conditions present when SiN_x layers are deposited onto c-Si by plasma enhanced vapour deposition. We examine how changing the width of the nitrogen gradient can affect a number of atomic level structural properties, which influence the optical and electrical performances of solar cells. We examine the trajectories of our simulations to search for certain geometries, which have previously been identified as being important at this interface. The number of silicon-silicon and silicon hydrogen bonds, which helps to determine the refractive index of the interface, is shown to increase with increasing N gradient width. The fixed charge in the interface is also shown to increase with the width of the gradient. The results demonstrate how altering the width of the N layer can affect the efficiency of a-SiN_x: H as both an anti-reflective coating and a passivation layer, and we suggest an optimal gradient width in the region of 2 nm. © 2012 American Institute of Physics. [http://dx.doi.org/10.1063/1.4764012]

I. INTRODUCTION

In order for high performance solar cells to attain everincreased efficiencies, one of the key considerations is an improvement in the lifetimes of charge carriers in the semiconductor. A major source of decreased carrier lifetimes is recombination of charge carriers at defects located at the semiconductor surface. For this reason, the topic of improved surface passivation has become one of the major areas of research in all areas of high-performance solar cell technology today. We investigate the use of amorphous silicon nitride (a-SiN $_x$), with a stoichiometric gradient at the crystalline silicon (c-Si) surface as an improved alternative to abrupt c-Si/SiN $_x$ interfaces.

The use of hydrogenated silicon nitride (SiN_x : H) represents one of the most important technological advances in solar cell technology. This is due to its ability to fulfil the dual roles of an anti-reflective coating (ARC) and surface passivation layer for crystalline silicon (c-Si).⁵ These SiN_x : H layers are commonly deposited on c-Si surfaces using plasma enhanced chemical vapour deposition (PECVD).⁶⁻⁸ a-SiN_x: H layers function as passivation layers by reducing the number of defective states at the c-Si surface, thus, lowering the recombination rate at the surface. It is also important that the ARC absorbs as little of the incident light as possible, for this reason, it is desirable that the SiN_x layer contains as few Si-Si and Si-H bonds as possible, as these bonds can absorb light in the region of the spectrum in which the solar cell is active.⁸

The electrical performance of a-SiNx passivation layers has been studied by means of deep-level-transient spectros-

copy (DLTS). $^{9-11}$ These studies reveal three different defect states (labeled A-C), which play a role at the Si-SiN $_x$ interface. Based on the DLTS measurements and theoretical analysis of the measured dependence of recombination rate on the excess carrier density, it was established that the defect labelled C dominates the recombination rate. 12 This defect has been identified as a Si centre bound to three N atoms with one dangling bond. This centre has also been identified as an important defect state in bulk a-SiN $_x$. 13 In accordance with common practice, this defect will be referred herein as the K-centre, see inset of Figure 1 for a graphical representation.

Another feature of the SiN_x layer which affects the electrical performance of a device is the presence of a positive fixed charge in the layer. The fixed positive charge in the SiN_x induces an inversion layer in the c-Si, which is highly conductive. It has been demonstrated that high values of Q_f in SiN_x result in improved effective surface recombination velocities. The major contribution to Q_f has been shown to be due to the presence of the K-centre. Thus, the K-centre has two contradictory roles in SiN_x passivation layers in solar cells. On one hand, it acts as a recombination centre, decreasing performance; on the other hand, it acts as a centre for fixed charge increasing performance.

The nature of the Si/SiN_x interface is very sensitive to the PECVD techniques and conditions used. For example, it is possible to have either a gradual interface, where the concentration of N has a gradient, going to zero over a finite distance from the bulk SiN_x to the c-Si, or a clean interface where there is an abrupt change from SiN_x to c-Si. In addition, the width of the gradual interface can be controlled by

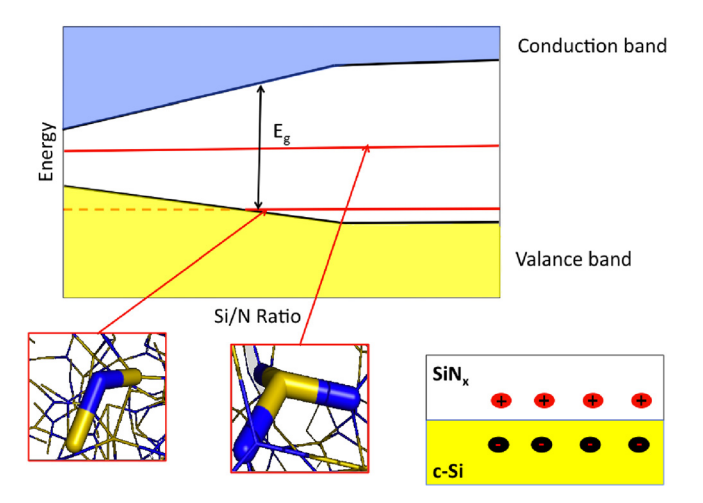


FIG. 1. (Top) Schematic representation of the SiN_x band structure as a function of the Si/N ratio. The red lines represent defect energy levels due to K- and N-defects. (Bottom left) The structure of the N-defect one N atom (blue), bonded to 2 Si atoms (yellow), with one dangling bond. (Bottom) Centre K-defect, one Si atom bonded to 3 N atoms with one dangling bond. (Bottom right) Representation of the formation of an inversion layer of negative charge in c-Si, due to fixed positive charge in the SiN_x layer.

the synthesis conditions. Previously, we have demonstrated how a graded Si/SiN_x interface, in which the concentration of N reduces gradually from the bulk value to zero at the interface, can result in a significant lowering of K-centre density at the interface. ¹⁷ We have also shown how it is possible to control the incorporation of N into the c-Si surface by a process of nitridation, ¹⁸ before deposition of the SiN_x : H layer. This allows for the introduction of a N gradient in the device, giving control of the Q_f and interface trap density, independent of the SiN_x : H layer.

In this paper, we provide a model for how the level of nitridation affects the important features of the ARC in a solar cell. We use a topological analysis of molecular dynamics (MD) simulations to investigate the effect of the gradient layer introduced by nitridation on the density of Si-Si and Si-H bonds, which are responsible for light absorption in the

ARC. We then estimate the fixed charge in the ARC, by calculating the density of K centres. Finally, we combine our model for defect distributions with Shockley-Reed-Hall (SRH) recombination statistics ^{19,20} to provide a model for how the carrier trapping rate is affected by the width of the N gradient layer introduced by nitridation.

II. COMPUTATIONAL METHODS

In order to represent the interaction between the atoms in our system, we have used the Tersoff potential, as parametrised by de Brito Mota *et al.*^{21,22} for hydrogenated silicon nitride. To generate amorphous SiN_x : H structures, we used a melt and quench methodology which we have verified previously. Starting from a random configuration of atoms in a simulation cell with dimensions chosen to match the experimental density of $SiN_{1.2}$, 3.10 g/cc. The random configuration is then run, using a timestep of 0.2 fs, for 0.5 ns at 2500 K in the canonical (NVT) ensemble to achieve a well equilibrated system. The system is then quenched to 350 K at a rate of 3×10^{11} K/s.

The amorphous sample generated is then placed in contact with the (111) surface of a slab of c-Si. To generate the gradient interface, we re-run the system again at 2500 K for 0.5 ns and quench to 350 K at the same rate. During this simulation, parts of the c-Si and a-SiN_{1.2}: H layers are held in a fixed position. In each case, the atoms allowed to move during the molecular dynamics simulation on either side of the interface are within half of the desired gradient interface width. The inter-diffusion of Si and N, which takes place during this step results in a N gradient across the desired width, represented schematically in Figure 2, which recreates the effects of nitridation before application of the a-SiN_{1.2}: H by PECVD experimentally. The final compositions of the simulation cells used in this study are presented in Table I.

In order to search for defects in our system, we have used the RINGS software package²³ to analyse the trajectories

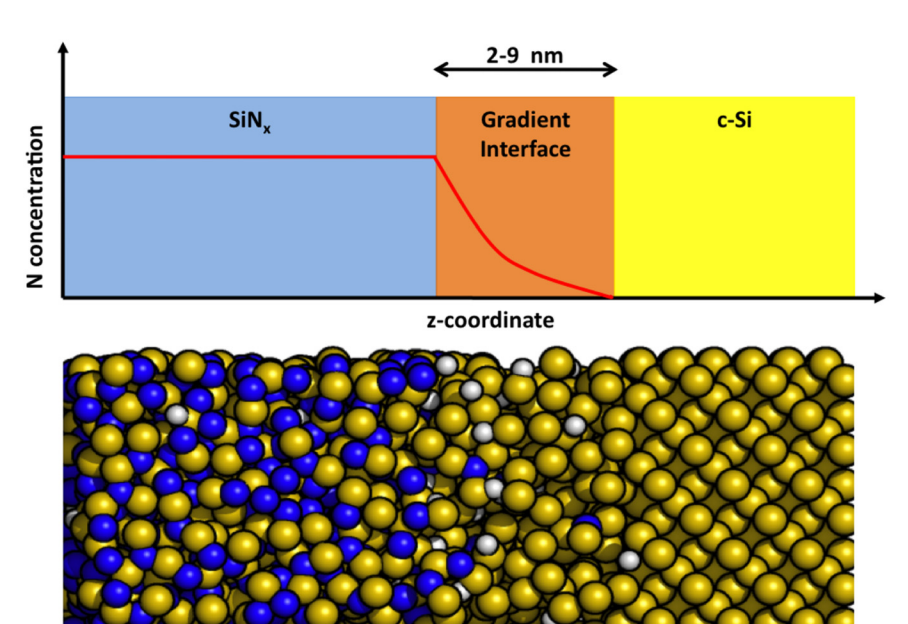


FIG. 2. System composition in our simulations. A layer of $SiN_{1.2}$ is on the left hand side of the system, this is linked to a layer of pure crystalline Si through a layer with a gradually reducing value of x in SiN_x . The width of the gradient interface layer is varied from 2 to 9 nm.

094303-3

TABLE I. Compositions of the cells used to create samples of a-SiN _x : H
for the different interface widths, showing number of Si, N, and H atoms
and the volume of the cell.

Sample (nm)	# Si	# N	# H	Volume/Å ³
2	406	487	99	9435.17
3	507	609	124	11793.96
4	609	730	149	14152.75
5	710	852	174	16511.54
6	811	974	198	18870.33
7	1095	913	223	21229.13
8	1014	1217	248	23587.92
9	1116	1339	273	25946.71

of our equilibrium MD simulations of the interfaces. Within this analysis, the coordination of an atomic centre is defined by the number of neighbouring atoms which are said to be "bonded" to that atom. The bonding is defined as the inter-atomic separation being within the first peak of the pair correlation function of the two atoms defined for a-SiN_x. Having, thus, defined the coordination of each atom, it is a simple task to count and map the defective centres in the simulation.

III. RESULTS AND DISCUSSION

A. Optical properties

The optical performance of SiN_x : H coated solar cells is affected adversely by light absorption in the ARC. In the case of SiN_x: H coatings, it is known that either Si-Si or Si-H bonds can be responsible for absorption. It is difficult to distinguish which is more responsible for light absorption. In Figure 3, we plot the dependence of both densities on the width of the N gradient at the c-Si interface. It is clear that wider nitridation gradients result in higher densities of Si-Si and Si-H bonds in the ARC. So when considering parasitic light absorption, it is clear that a narrower nitridation layer is favourable. In addition, the refractive index (n) of SiN_x : H

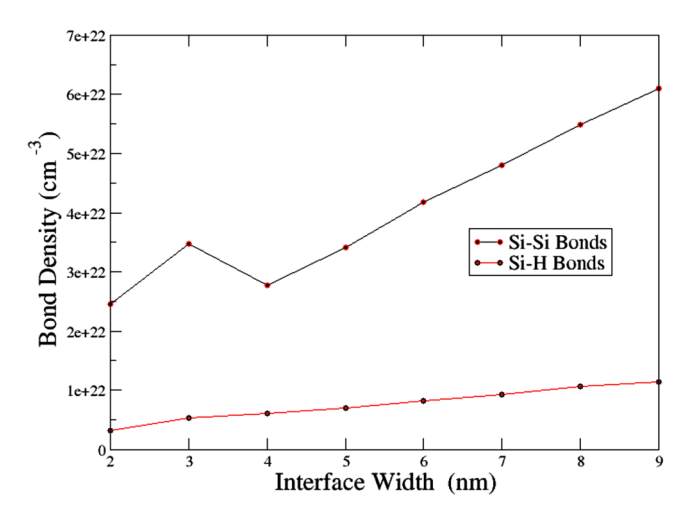


FIG. 3. Density of silicon-silicon and silicon hydrogen bonds and percentage of silicon centres which have the geometry corresponding to the K-centre defect, as a function of the width of the N density gradient at the a-SiN_x: H/c-Si interface.

on c-Si is known to be related to either the concentration of Si-H or Si-Si bonds. Whilst it is again difficult to determine which of the bond densities is more important, since our analysis reveals that they are correlated to one another and also to the gradient width, optimization of n could, in principle, be achieved by tuning the gradient width. We will now consider other properties of the SiN_r: H layer which are more related to the electronic properties of the cell.

B. Fixed charge

As we explained in the Introduction, the presence of a fixed charge (Q_f) in the SiN_x : H layer is desirable as it reduces the minority carrier density in the c-Si interface region, thus, reducing the recombination rate and increasing the majority carrier lifetime. In this section, we will consider how the nitridation profile affects the fixed charge. The fixed charge in Si-SiN_x interfaces has been shown to consist of a constant contribution from oxygen correlated states and an operating condition dependent contribution due to K⁺ centres.^{5,12} In this study, we are considering the effects of different levels of nitridation, therefore, we consider only the latter contribution to Q_f . We analyse the trajectories of our MD simulations to identify K centres, which are defined as under coordinated Si centres bonded to three N atoms. We define Si-N and Si-Si bonds based on the first peak of the pair correlation functions, as described in a previous study. 17 The region in which the fixed charge of the SiN_x : H layer is important has been shown to be around 20 nm. In our samples, the bulk region of $SiN_x 1.2$: H will have the same density of fixed charge in each system, thus, any differences will be due to different levels of fixed charge in the gradient region. For this reason, we consider only the first 9 nm of the SiN_x : H layer in all of our samples in this analysis, since the remainder of the SiN_x : H will be the same from the point of view of Q_f concentration. The results are presented in Figure 4.

We can see from Figure 4 that there is a peak in the number of K centres at an interface width between 2 and 3 nm. We note that not all K centres will be positively charged and contributing to the fixed charge in the SiN_x layer; therefore, our analysis does not provide an absolute

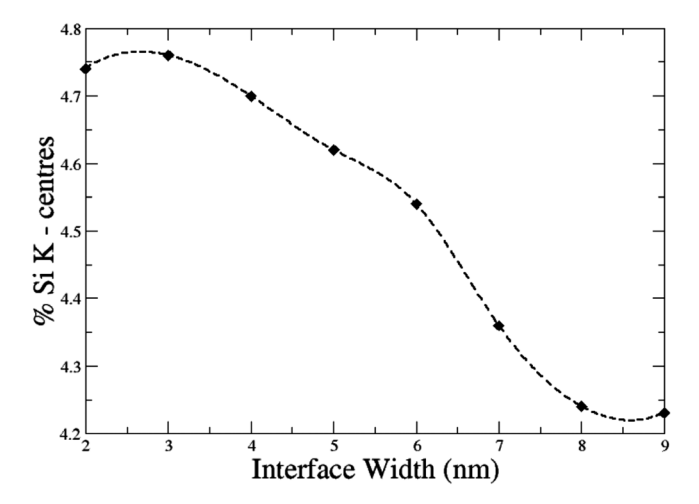


FIG. 4. The percentage of Si atoms which have K centre topology as a function of the width of the N gradient region.

value for the value of Q_f . However, we think that it is reasonable to assume that the greater the number of K centres the higher the fixed charge will be under otherwise identical circumstances. Thus, the comparison of the number of K centres in the various systems gives an indication of how much they will contribute relatively to the fixed charge. Our simulations show that too heavy nitridation, resulting in an interface width of greater than 3 nm, would be expected to reduce the fixed charge.

C. Trap density

We now consider how the distribution of defects is affected by the gradient at the interface. Figure 5 shows how the distribution of two important defects in the a-SiNx: H layer depends on the width of the layer of a-SiN_x: H. It has been shown⁸ that increased trap state densities (D_{it}) at the semiconductor/insulator interface result in reduced carrier lifetimes. Thus, it is desirable to minimise D_{it} at the interface in order to improve device performance. Figure 5 plots the density of K-centre defects mentioned previously across the various interfaces. Clearly, from this figure the wider interface gradients lead to a reduction of the K centre density at the interface. Figure 5 plots the density of N centres with a dangling bond, which have also been identified as possible trap states in a-SiN_x. ^{24,25} Again the density of these defects close to the interface is reduced when the interface gradient is increased.

D. Effects of the gradient interface on recombination

We now present a simplified model, based on our calculated trap densities, and estimations of the carrier concentrations, of the degree to which we would expect recombination to occur in the various gradient interfaces.

As Si is an indirect bandgap semiconductor, the dominant source of recombination will be bulk traps. Recombination can be considered as a process of electron and hole capture, which can be described by SRH statistics.¹⁹

According to the SRH model, the rate of capture is given by

$$U = \left[1 - \exp\frac{E_t - E_n}{k_B T}\right] f_{pt} \rho_T \times \int_{e_c}^{\infty} f(E) N(E) c_n(E) dE. \quad (1)$$

Here, E_t is the energy of the trap and E_n is the quasi Fermi level. We consider the system under the condition of zero bias, where the quasi-Fermi level is equal to the intrinsic Fermi level (E_{F_n}), and is located almost at mid-gap for non-doped systems. f_{pt} is the probability that a trap is empty (thus available to any carrier) and ρ_T is the trap density. The integral runs from the bottom of the conduction band (e_c) to all higher levels and the terms in the integrand are the fraction of states occupied by electrons (f(E)), the number of quantum states (N(E)), and the probability per unit time that an electron will be trapped by a given trap ($c_n(E)$). In our analysis, we replace the integral of f(E) N(E) dE by a carrier density ρ_n . The density of carriers, in a non-degenerate n-type semiconductor, is given by e^{26}

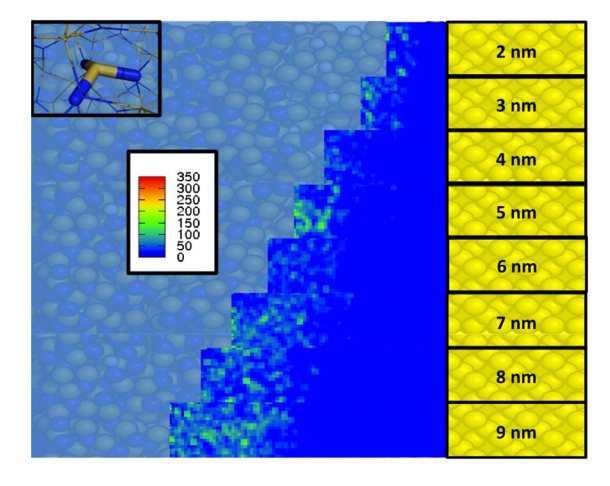
$$\rho_n = 2\left(\frac{2\pi m_{de}k_BT}{h^2}\right) \exp\left(\frac{-E_{F_n} - E_V}{k_BT}\right),\tag{2}$$

where E_V is the energy of the valence band minimum. Since the Fermi energy for an intrinsic semiconductor lies very close to the middle of the band gap, and as we do not expect the SiN_x layer to have a significant dopant population, we estimate the value $E_{F_n} - E_V$ to be half of the band gap. m_{de} is the effective mass of an electron in the conduction band.

Therefore, we re-write Eq. (1) as

$$U = \left[1 - \exp\frac{E_t - E_n}{k_B T}\right] f_{pt} \rho_T \rho_n \times \int_{e_n}^{\infty} c_n(E) dE.$$
 (3)

The value for m_{de} in c-Si is $0.33m_e$ (Ref. 26) and that in SiN_x is $\sim 0.5m_e$. The variation of the band gap of SiN_x with stoichiometry has been calculated by Robertson. In Figure 6, we present the variation of the band gap with



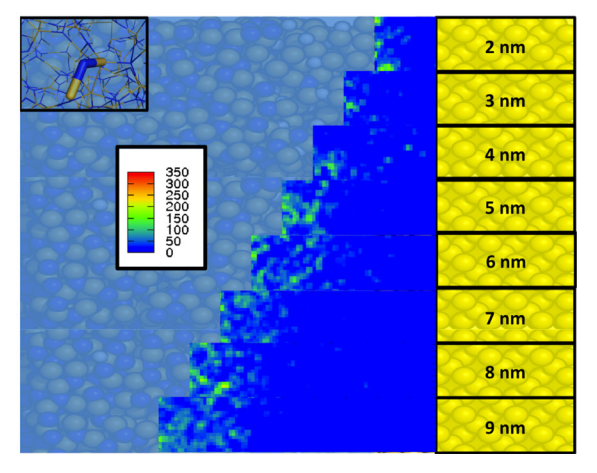


FIG. 5. Plots of the density of important geometrical defects across the gradient layer in the a-SiN_x: H/c-Si interface. The graph shows (vertical) gradients with widths from 2 nm (top) to 9 nm (bottom). x = 1.2 in SiN_x (light blue region to the left) and decreases linearly to x = 0 on the right (c-Si interface) for each width. The left plot shows K-centre density, the right plot shows N-centre density. Insets on each plot show a graphical representation of the defect in question; the legends show the number of instances of the defect centre in each volume region during the MD simulation.

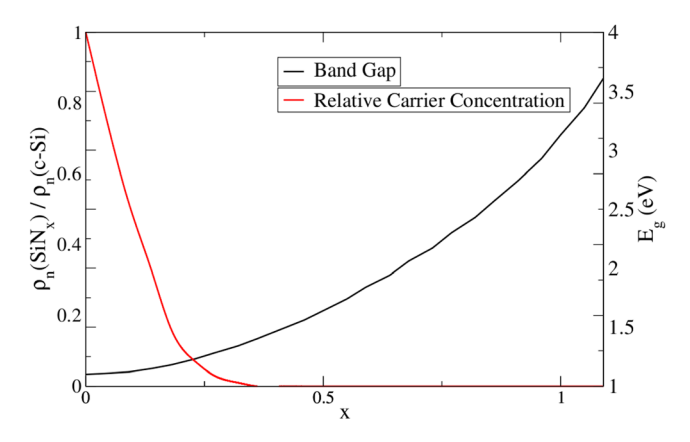


FIG. 6. Band gap dependence on the stoichiometry of SiN_x , as calculated by Robertson, ³⁰ and the resultant electron carrier population normalised by the carrier population in pure c-Si, calculated from Eq. (2).

stoichiometry and the resultant variation in carrier concentration in the SiN_x layer as calculated using Eq. (2).

The trap density is then calculated from the trajectories of the MD simulations, with the active trap density defined as

$$\rho_T(z) = \rho_K(z) + \rho_N(z)\delta, \quad \delta = \begin{cases} 1 & \text{if } x \ge 1, \\ 0 & \text{if } x < 1, \end{cases}$$
 (4)

where $\rho_K(z)$ is the density of K centres not passivated by hydrogen, $\rho_N(z)$ is the density of N centres not passivated by hydrogen and the delta function is 1 when x in SiN_x is greater than 1 and 0 when x is less than 1, to reflect the fact that below x=1, the N centre is no longer active in the band gap of SiN_x as illustrated in Figure 1. This predicts very little contribution to trapping from N centres in the gradient interface, since by the time the band gap is wide enough for the N-centre to be active, the carrier population is vanishingly small. Thus, we ignore the contribution from N centres to trapping in gradient interface systems. The rate of capture at the K centre will depend on the difference between E_t and E_n in Eq. (1), as we have already stated $E_n = E_{F_n}$ at zero bias. Since E_{F_n} is located at almost mid-gap as is E_t for the K

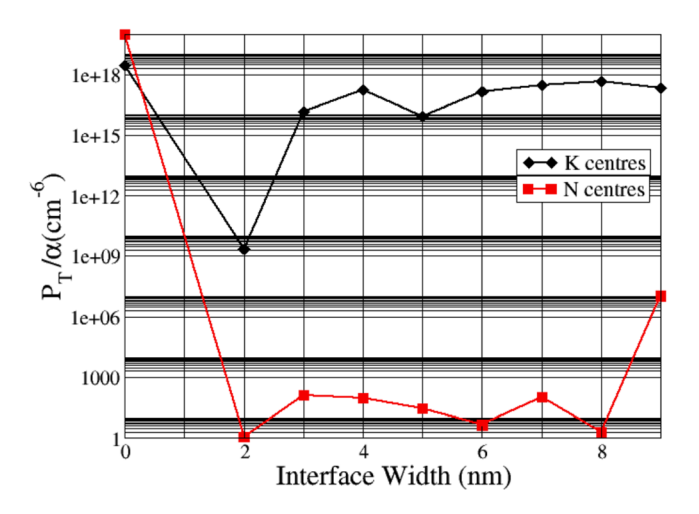


FIG. 7. Probabilities of carrier trapping at defect centres depending on interface gradient thickness, calculated from Eq. (5).

centre, 31 and given that the band gap opens almost symmetrically about mid-gap 30 across the SiN $_x$ composition range, this dependence will not change across the composition range either. Thus, we can say that the probability of a carrier being trapped will be proportional to the trap density and the carrier density in the system.

$$P_T = \alpha \int_0^Z \rho_T(z) \rho_n(z) dz, \tag{5}$$

where the integral is calculated from the c-Si/SiN_x interface at zero, to the edge of the SiN_x layer at Z. The constant of proportionality is

$$\alpha = \left[1 - \exp\frac{E_t - E_n}{k_B T}\right] f_{pt} \int_{e_r}^{\infty} c_n(E) dE, \tag{6}$$

and does not change across the composition range. P_T/α for the various interface widths at zero bias is plotted in Figure 7.

As can be seen from Figure 7, the introduction of a gradient interface results in a significant drop in the trapping probability for both N and K centres. The number of N centre traps drops to almost zero, implying that N centres will play almost no role as recombination centres in gradient interface systems. The trapping probability for K centres begins to rise again, by three orders of magnitude, with the introduction of a gradient wider than 2 nm. Given our earlier findings regarding the relationship between fixed charge, optical properties, and the gradient width, our simulations suggest that a gradient introduced by nitridation can have a beneficial effect on the performance of a solar cell, but that the degree of nitridation should be limited and an optimal width of the gradient region is around 2 nm.

IV. CONCLUSIONS

In conclusion, we have performed molecular dynamics simulations to investigate the effect of a N density depletion layer at the interface between c-Si and a-SiN $_x$: H. In particular, we have concentrated on how the width of the depletion layer affects the density and distribution of a number of bond types and defect states which have previously been shown to be important for the performance of solar cells when a-SiN $_x$ is used as an ARC.

By considering the density of Si-Si and Si-H bonds, the density of K-centre defects, and the locations of K- and N-centre defects, we believe that these results suggest that a gradual interface with a gradient in ρ_N can be designed to improve device efficiency. Furthermore, we believe that the results suggest that there should be an optimal width of the ρ_N gradient, which would result in the best balance between layer stability, fixed charge, and concentration of recombination centres at the interface. Although we realise that the complexity of the factors which affect operational solar cells means that we can only consider a small number of important aspects, we believe that our simulations suggest that an a-SiN_x gradient layer of around 2 nm would provide the

best compromise between layer stability and electrical performance.

ACKNOWLEDGMENTS

The authors acknowledge support from the European Commission grant MMP3-SL-2009-228513, "Hipersol" as part of the 7th Framework package, Grant No. 228513. Via our membership of the UK's HPC Materials Chemistry Consortium, which is funded by EPSRC (EP/F067496), this work made use of the facilities of HECToR, the UK's national high-performance computing service, which is provided by UoE HPCx Ltd at the University of Edinburgh, Cray Inc, and NAG Ltd, and funded by the Office of Science and Technology through EPSRC's High End Computing Programme.

- ¹D. R. Kim, C. H. Lee, P. M. Rao, I. S. Cho, and X. Zheng, Nano Lett. 11, 2704 (2011).
- ²C.-F. Chi, P. Chen, Y.-L. Lee, I.-P. Liu, S.-C. Chou, X.-L. Zhang, and U. Bach, J. Mater. Chem. **21**, 17534 (2011).
- ³Y. Dan, K. Seo, K. Takei, J. H. Meza, A. Javey, and K. B. Crozier, Nano Lett. **11**, 2527 (2011).
- ⁴H. Lee, T. Tachibana, N. Ikeno, H. Hashiguchi, K. Arafune, H. Yoshida, S. ichi Satoh, T. Chikyow, and A. Ogura, Appl. Phys. Lett. **100**, 143901 (2012).
- ⁵A. G. Aberle, Sol. Energy Mater. Sol. Cells **65**, 239 (2001).
- ⁶R. Hezel and R. Schroner, J. Appl. Phys. **52**, 3076 (1981).
- ⁷R. Hezel and K. Jaeger, J. Electrochem. Soc. **136**, 518 (1989).
- ⁸S. Jung, D. Gong, and J. Yi, Sol. Energy Mater. Sol. Cells **95**, 546 (2011).

- ⁹A. G. Aberle, S. Glunz, and W. Warta, J. Appl. Phys. **71**, 4422 (1992).
- ¹⁰J. Schmidt, F. M. Schuurmans, W. C. Sinke, S. W. Glunz, and A. G. Aberle, Appl. Phys. Lett. 71, 252 (1997).
- ¹¹C. Gong, E. Simoen, N. Posthuma, E. V. Kerschaver, J. Poortmans, and R. Mertens, Appl. Phys. Lett. 96, 103507 (2010).
- ¹²J. Schmidt and A. G. Aberle, J. Appl. Phys. **85**, 3626 (1999).
- ¹³P. M. Lenahan and S. E. Curry, Appl. Phys. Lett. **56**, 157 (1990).
- ¹⁴R. Hezel, Solid-State Electron. **24**, 863 (1981).
- ¹⁵J.-F. Lelièvre, E. Fourmond, A. Kaminski, O. Palais, D. Ballutaud, and M. Lemiti, Sol. Energy Mater. Sol. Cells 93, 1281 (2009).
- ¹⁶H. Mackel and R. Ludemann, J. Appl. Phys. **92**, 2602 (2002).
- ¹⁷K. T. Butler, M. P. W. E. Lamers, A. W. Weeber, and J. H. Harding, J. Appl. Phys. **110**, 124905 (2011).
- ¹⁸M. W. P. E. Lamers, K. T. Butler, J. H. Harding, and A. Weeber, Solar Energy Mater. Sol. Cells **106**, 17 (2012).
- ¹⁹W. Shockley and W. T. Read, Phys. Rev. **87**, 835 (1952).
- ²⁰R. N. Hall, Phys. Rev. **87**, 387 (1952).
- ²¹F. de Brito Mota, J. F. Justo, and A. Fazzio, Phys. Rev. B **58**, 8323 (1998).
- ²²F. de Brito Mota, J. F. Justo, and A. Fazzio, J. Appl. Phys. 86, 1843 (1999).
- ²³S. L. Roux and P. Jund, Comput. Mater. Sci. **49**, 70 (2010).
- ²⁴W. L. Warren, P. M. Lenahan, and S. E. Curry, Phys. Rev. Lett. 65, 207 (1990).
- ²⁵G. Pacchioni and D. Erbetta, Phys. Rev. B **60**, 12617 (1999).
- ²⁶Physics, Applications of Semiconductor Microstructures, edited by M. Jaros (Oxford Science, New York, 1989).
- ²⁷V. A. Gritsenko, E. E. Meerson, and Y. N. Morokov, Phys. Rev. B 57, R2081 (1998).
- ²⁸K. Nasyrov, V. Gritsenko, M. Kim, H. Chae, S. Chae, W. Ryu, J. Sok, J.-W. Lee, and B. Kim, IEEE Electron Device Lett. 23, 336 (2002).
- ²⁹Y. Shi, X. Wang, and T.-P. Ma, IEEE Trans. Electron Devices **46**, 362 (1999).
- ³⁰J. Robertson, Philos. Mag. B **63**, 47 (1991).
- ³¹J. Robertson, Philos. Mag. B **69**, 307 (1994).